Oil & Natural Gas Technology

DOE Award No.: DE-FE0013531

Quarterly Research Performance

Progress Report (Period Ending 03/31/2018)

Project Title

Assessing the response of methane hydrates to environmental change at the Svalbard continental margin

Project Period (11/1/2013 to 10/31/2018)

Submitted by:
Marta E. Torres

Oregon State University
DUNS #: 053599908
104 CEOAS Admin. Bldg.
Corvallis, OR 97331-5503
Email: mtorres@coas.oregonstate.edu
Phone number : (541) 737-2902

Prepared for:
United States Department of Energy
National Energy Technology Laboratory

Submission Date

U.S. DEPARTMENT OF ENERGY | NATIONAL ENERGY TECHNOLOGY LABORATORY

Office of Fossil Energy

EXECUTIVE SUMMARY

In November 2013, Oregon State University initiated the project entitled: **Assessing the response of methane hydrates to environmental change at the Svalbard continental margin.** In this project, we will take advantage of a unique opportunity to collect samples from the Svalbard continental margin. The overall objective of this research is to constrain the biogeochemical response of the gas hydrate system on the Svalbard margin to environmental change. Because of a delay in the planned expedition, we reconfigured the program based on discussions with NETL program managers and submitted a revised SOPO. In the new plan, we collected samples in six expeditions: RV Helmer Hanssen, Oct., 2014; RV Helmer Hanssen, May, 2015; RV Heincke, July-August 2015 and August-Sept, 2015; RV Helmer Hanssen, June 2016, and MeBo drilling expedition in August-September, 2016.

The very productive outcome of this collaboration is evidenced on six papers published in highly ranked journals, with 2 more in preparation; two articles in the Fire in the Ice magazine; and more than 15 presentations at science conferences and meetings.

PROGRESS, RESULTS, AND DISCUSSION

1. Water column results. Water column analyses are completed and resulted in one publication in the journal "Scientific Reports" (www.nature.com/scientificreports) doi:10.1038/srep42997. And in an article in the FITI magazine (attached). These results were presented at two international conferences: Gordon Research Conference (Galveston, March 2016) and ICGH (Denver, June 2017).

2. Geochemistry: Geochemical analyses of cores is generating lots of data to constrain fluid flow and gas hydrate formation in the margin. A first paper detailing results from the gas hydrate mounds region was published in the journal Nature Communications on 7th June 2017(http://www.nature.com/ncomms) doi: 10.1038/NCOMMS15745. These results were presented in two international conferences: Gordon Conference on Natural Gas Hydrates March, 2016; and Gas In Marine Sediments conference to be held in Tromsoe, September 2016. Follow-up on this first paper continues, data was presented presentations at Goldschmidt Conference, Paris Aug 2017. New results from gas transport in fractures in a seep of Vestnesa Ridge is in progress, with preliminary results being presented in the upcoming EGU general assembly 2018. In addition, a new manuscript has been accepted for publication in Geophysical Research Letters (manuscript 2018GL077309R). In this paper we document decoupled methane transport by gaseous and aqueous phases in Storfjordrenna (offshore Svalbard) and propose a three-stage evolution model for active seepage in the region where gas hydrates are present in the shallow subsurface. In a pre-active seepage stage, solute diffusion is the primary transport mechanism for methane in the dissolved phase. Fluids containing dissolved methane have high $^{87}Sr/^{86}Sr$ ratios due to silicate weathering in the microbial methanogenesis zone. During the active seepage stage, migration of gaseous methane results in near-seafloor gas hydrate formation and vigorous seafloor gas discharge with a thermogenic fingerprint. In the post-active seepage stage, the high concentration of dissolved lithium points to the contribution of a deeper-sourced aqueous fluid, which we postulate advects upward following cessation of gas discharge.

3. Data integration/synthesis for the Vestnesa seeps. Based on collaborations with Norwegian colleagues, a synthesis of the data collected during various cruises to the Vestnesa Ridge, were integrated in a manuscript published in Marine Geology (Panieri et al., 2017. This synthesis include results from the CAGE15-5 expedition in which I participated, and which was highlighted in a FITI article in 2015.

4. MSM57 expedition (29 July-07 September, 2016). Sample and data analyses from drilling expedition using the MeBo seafloor drill are underway. Results from samples offshore Prinz Karl Forland were presented at the ICGH in 2017, an a manuscript is now published in Nature Communications. Sediment cores drilled off Prinz Karls Foreland contain freshwater from dissociating hydrates. However, our modeling indicates that the observed pore water freshening began around 8 ka BP when the rate of isostatic uplift outpaced eustatic sea-level rise. The resultant local shallowing and lowering of hydrostatic pressure forced gas hydrate dissociation and dissolved chloride depletions consistent with our geochemical analysis. Hence, we propose that hydrate dissociation was triggered by postglacial isostatic rebound rather than anthropogenic warming. Gas hydrate acts as a dynamic seal that regulates methane release from deep geological reservoirs. Hydrocarbon data recovered by drilling on Vestensa Ridge, was presented at the upcoming GeoBremen2017. Since we have generated more data on the isotopic composition of carbon in aqueous and gas phases in support of a manuscript in progress.

5. Microbiology incubations: A timeseries of incubations spanning several months was carried out on sediments collected from two regions overlying methane hydrates and one methane-free reference from CAGE cruise 16-5 (June-July 2016). Preliminary results are summarized in the Appendix, and are the topic of a dissertation for doctoral candidate Scott Klasek. These results were presented at the upcoming Ocean Sciences Meeting, Portland 2018.

1. PROBLEMS OR DELAYS

No delays or problems during this quarter

PRODUCTS

- Two papers published on numerical model aspects of the project. Full citations:
  Peszynska, M., Medina, F.P., Hong, W.L. and Torres, M.E., 2015. Reduced Numerical Model for Methane Hydrate Formation under Conditions of Variable Salinity. Time-Stepping Variants and Sensitivity. Computation, 4(1), p.1.

  Peszynska, M., Hong, W.L. Torres, M.E., and Kim, J-H., 2015. Methane Hydrate Formation in Ulleung Basin Under Conditions of Variable Salinity: Reduced Model and Experiments. Transport Porous Media DOI 10.1007/s11242-016-0706-y

- A paper published in Nature-Scientific Reports with water column results.
  Mau, S., Römer, M., Torres, M.E., Bussmann, I., Pape, T., Damm, E., Geprägs, P., Wintersteller, P., Hsu, C.W., Loher, M. and Bohrmann, G., 2017. Widespread methane seepage along the continental margin off Svalbard-from Bjørnøya to Kongsfjorden. Scientific Reports, 7.

- A paper published in Nature Communications on the gas hydrate mounds.

Hong, W. L., Torres, M. E., Carroll, J., Crémière, A., Panieri, G., Yao, H., & Serov, P. (2017). Seepage from an arctic shallow marine gas hydrate reservoir is insensitive to momentary ocean warming. Nature communications, 8, 15745.10.1038/NCOMMS15745.

- A synthesis paper on Vestnesa Ridge published in Marine Geology:
  Panieri G, Bünz S, Fornari DJ, Escartin J, Serov P, Jansson P, Torres ME, Johnson JE, Hong W, Sauer S, Garcia R. An integrated view of the methane system in the pockmarks at Vestnesa Ridge, 79° N. Marine Geology. 2017 Aug 1;390:282-300.

- A paper published in Nature Communications on PKF hydrate dissociation by isostatic rebound:
  Wallmann K, Riedel M, Hong WL, Patton H, Hubbard A, Pape T, Hsu CW, Schmidt C, Johnson JE, Torres ME, Andreassen K. Gas hydrate dissociation off Svalbard induced by isostatic rebound rather than global warming. Nature communications. 2018 Jan 8;9(1):83.

- A paper in press in Geophysical Research Letters by W.-L. Hong, M.E. Torres, A. Portnov. M. Waage, B. Haley, and A. Lepland, Variations in gas and water pulses at an Arctic seep: fluid sources and methane transport. 2018. (attached)

- Abstracts submitted since the last quarterly report: Ocean Sciences meeting, Portland Feb. 2018 and the EGU General Assembly, April 2018 Vienna

Variations in gas and water pulses at an Arctic seep: fluid sources and methane transport

W.-L. Hong[1,2*], M.E. Torres[3], A. Portnov [2,4], M. Waage[2], B. Haley[3], and A. Lepland[1]

[1]Geological Survey of Norway, Trondheim, Norway

[2]Centre for Arctic Gas Hydrate, Environment and Climate, the Arctic University of Norway (UiT), Tromsø, Norway

[3]College of Earth, Ocean, and Atmospheric Sciences, Oregon State University, Corvallis, OR, USA

[4]School of Earth Sciences, Ohio State University, OH, USA

*Corresponding author: W.-L. Hong (Wei-Li.Hong@NGU.no)

Key Points (140 characters each):

- We document the decoupled gaseous and aqueous fluid phases from Storfjordrenna, a cold seep south of Svalbard.
- We propose a three-stage evolution model with different modes of methane transport in each stage.
- The evolution of the seepage is controlled by the availability of gaseous methane and/or the development of fluid conduits.

Abstract

Methane fluxes into the oceans are largely dependent on the methane phase as it migrates upward through the sediments. Here we document decoupled methane transport by gaseous and aqueous phases in Storfjordrenna (offshore Svalbard) and propose a three-stage evolution model for active seepage in the region where gas hydrates are present in the shallow subsurface. In a pre-active seepage stage, solute diffusion is the primary transport mechanism for methane in the dissolved phase. Fluids containing dissolved methane have high $^{87}Sr/^{86}Sr$ ratios due to silicate weathering in the microbial methanogenesis zone. During the active seepage stage, migration of gaseous methane results in near-seafloor gas hydrate formation and vigorous seafloor gas discharge with a thermogenic fingerprint. In the post-active seepage stage, the high concentration of dissolved lithium points to the contribution of a deeper-sourced aqueous fluid, which we postulate advects upward following cessation of gas discharge.

1. Introduction

Continental margin sediments constitute the largest known natural hydrocarbon source to the global ocean (Hovland et al., 1993; Kvenvolden and Rogers 2005; Reeburgh 2007). Methane emission at the seafloor necessitates transport through the sediment either in the gas phase or as a dissolved constituent in porewater. Dissolved methane migrates by diffusion and/or it can be transported with the aqueous phase (i.e., advection). Most of the dissolved methane is consumed by microorganisms within the upper few meters of sediments through aerobic and anaerobic oxidation of methane (AeOM and AOM, respectively) (Boetius and Wenzhofer 2013), which limit methane escape to the overlying water column (Regnier et al., 2011). Microorganisms cannot utilize methane in the gas phase; therefore, in areas of intense upward fluid migration, where the methane concentration exceeds solubility, methane gas bypasses the microbial filter and escapes into the water column. Methane bubbling into the water column from the seafloor have been widely documented through direct observations (MacDonald et al., 1994; Haeckel et al., 2004; Sauter et al., 2006; Sahling et al., 2014) as well as by hydrocasts and hydroacoustic surveys (Nikolovska et al., 2008; Greinert et al., 2010; Römer et al., 2012; Greinert et al., 2013; Smith et al., 2014; Mau et al., 2017).

Here we report on porewater geochemistry and geophysical observations from a recently described field of gas hydrate mounds (GHMs) in the Storfjordrenna Trough Mouth Fan, south of Svalbard (Fig. 1a&1b). Persistent hydroacoustic anomalies were detected in the water column above four of the surveyed GHMs (Serov et al., 2017), and abundant gas hydrates were recovered in the sediments of these features by gravity coring (Hong et al., 2017). GHM5 is the exception, as from this mound there are neither hydroacoustic anomalies nor gas hydrates, despite its close proximity (<1 km) to other GHMs. We mapped the distribution of gas-related amplitude anomalies in 3D seismic data and inferred the origin of methane gas from its stable isotopic signatures. These data were combined with results of porewater geochemistry analyses to infer sources of the aqueous phase and water-rock interactions. Based on these results, we hypothesize that the observed contrasting seepage activity reflects the different evolutionary stages of the system, controlled by the transport of different fluid phases (i.e., gas versus water). Our observations provide critical constraints for the fluid migration within this shallow water Arctic gas hydrate field, which serve as an example for other cold seeps along continental margins worldwide.

2. **Geological setting and site description**

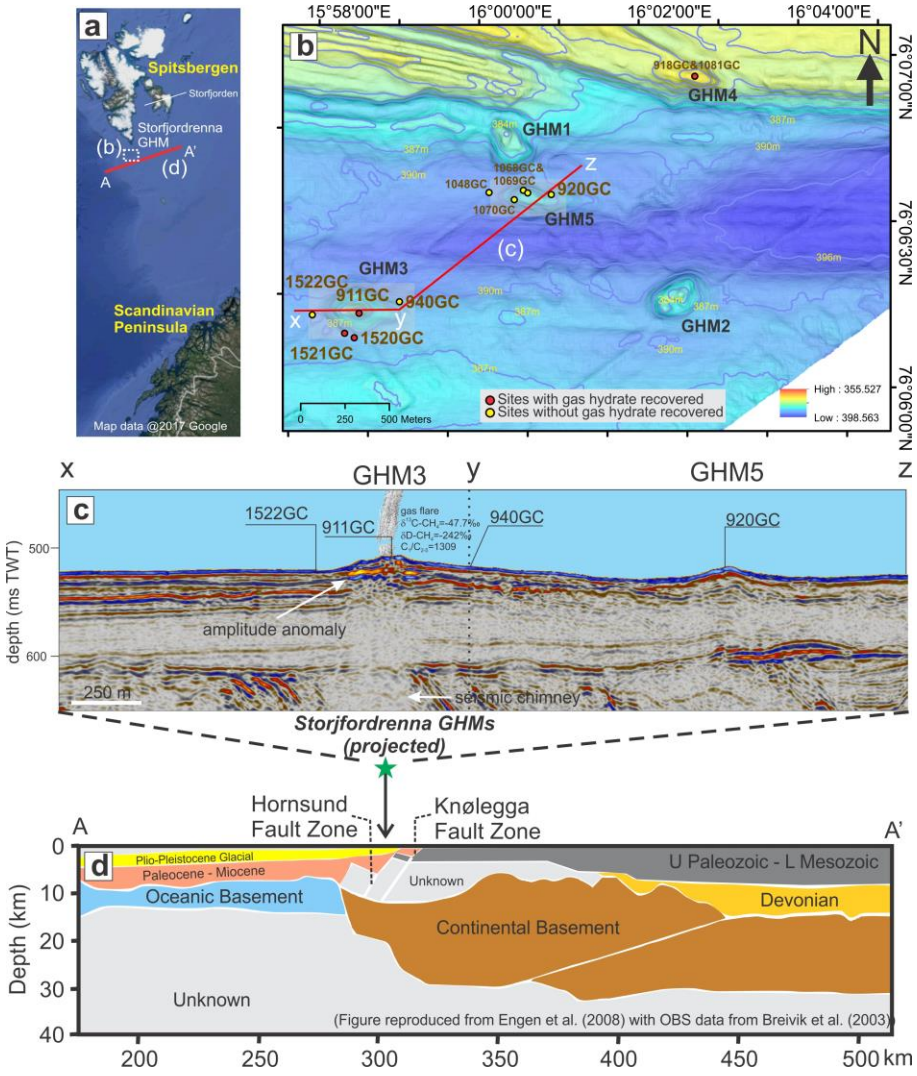

Figure 1: (a) A regional map showing the study area and the location of the deep seismic profile in (d). (b) Detailed bathymetry map showing the investigated sediment cores. We focused on the completed dataset from the six sites (larger label fonts in (b)) and showed available data for the other six sites (smaller label fonts in (b)) in the Supplementary information. The red line (x-y-z) marks the location of the P-Cable seismic line in (c) across the two investigated GHMs with the stable isotopic signatures of a gas bubble sample collected. (d) Structural geological profile (modified after Engen et al., 2008) showing the location of the two major fault systems in relation to Storfjordrenna GHMs.

The Storfjordrenna GHMs are located ~50 km south of Spitsbergen at ~390 m water depth (Fig. 1b). Two major fault systems cut across this region: the Hornsund Fault Zone (HFZ) (also known as De Geer Fracture Zone) and the Knølegga Fault Complex (KFC) (Fig. 1d). The HFZ is located at the western edge of the continental basement, adjacent to the continent-ocean

boundary (Breivik et al., 2003). To the east of HFZ, the sub-parallel development of the KFC represents the down-faulted terrace of the continental crust which is considered as a part of the Hornsund fault complex (Sundvor and Eldholm 1976; Myhre et al., 1982; Gabrielsen 1984). The HFZ was proposed to serve as a pathway for methane transport, based on multiple gas seepage sites observed from 72^{o} to 79^{o} N that coincide with this structural lineament (Mau et al., 2017).

Glacial cycles in this region have strongly modulated sediment transport, seafloor topography, and the sub-seafloor pressure regime (Ingólfsson and Landvik 2013; Wegner et al., 2015; Patton et al., 2016). Repeated glaciations led to alternation of depositional and erosional processes which in the Storfjordrenna region is reflected in a ~50-150 m thick upper glacial unit (Elverhøi and Solheim 1983). In addition, isostatic adjustment associated with deglaciation (Patton et al., 2016) has been shown to play an important role in the reactivation of faults and the seismicity of the region, which also in turn facilitate fluid migration (Mörner 1978; Stewart et al., 2000).

In our study area, minerals in the glacial/glacial-marine clays and silts are mainly composed of quartz (20-40%), feldspar (5-15%), carbonates (10-20%) and clay minerals (Andersen et al., 1996). As documented in Hong et al. (2017), cores recovered from the GHMs contain abundant methane-derived authigenic carbonate nodules. At sites with active gas discharge, gas hydrates occurred as shallow as 0.85 meters below seafloor (mbsf). Datings of two planktonic foraminifera specimens from a 3.2 m long gravity core without any sign of active methane discharge (1522GC in Fig. 1b) yield an age for the bottom of this core slightly older than 16.2 kyrBP whereas the upper 70 cm is of Holocene age (Hong et al., 2017).

3. Methods

Sampling and analytical methods for porewater and gas samples are detailed in the Supplementary information with data included in the Dataset S1. The seismic data used in this study were obtained during a 3D seismic P-Cable survey in 2016, which generated a broadband high-resolution dataset (6.25 × 6.25m bin size) suitable for mapping geological structures in the shallow subsurface (<1000mbsf). Details of data acquisition and processing are given in Petersen et al. (2010) and Waage et al. (in prep). The seismic data is being examined to further investigate the geological settings and the controls of seepage in the area (Waage et al., in prep).

4. Results and Discussion

Porewater data from the six investigated sites are presented in Fig. 2 (See Table S1 of the Supporting information for site location and water depths). We included the available data from six additional sites (labeled with smaller fonts in Fig. 1) in the Supplementary material to generalize our observations. However, as the dataset is not as complete in these six additional sites as in the others, we will not focus our discussion on them. In general, sulfate concentrations decrease with depth either in a monotonic (1522GC and 920GC) or in a non-linear fashion (911GC, 940GC, 1520GC, and 1521GC). After considering various processes that can lead to non-steady-state porewater profiles, Hong et al. (2017) concluded that such porewater profiles result from a recent increase in methane flux. Also, aqueous advection is insignificant at the active sites despite the shallow (<1 mbsf) sulfate-methane-transition-zone (SMTZ). Rather, diffusion of methane from a shallow fluid flow system, as seen from the seismic profile (Fig. 1c), sustains the high AOM rates observed from these sites.

Chloride concentrations are close to the seawater value (558 mM) at most sites, with downcore increasing and decreasing trends observed in 920GC and 1522GC, respectively (Fig. 2). It is well-established that gas hydrate dissociation during core recovery can dilute the concentrations of all ions including chloride while rapid gas hydrate formation can result in chloride content higher than the seawater value (Ussler and Paull 2001; Haeckel et al., 2004; Torres et al., 2004; Torres et al., 2011). However, there is no sufficient methane flux to sustain gas hydrate formation at GC920 and GC1522 (Serov et al., 2017) and consequently no recovery gas hydrate was recovered from either site (Hong et al., 2017). Therefore, we are confident that the observed chloride variations at 920GC and 1522GC are not related to gas hydrate dissociation and/or formation. Other potential freshening sources include dehydration of clay minerals at depth (Kastner et al., 1991; Kim et al., 2013a), clay membrane ion filtration (Haydon and Graf 1986), and/or mixing of a meteoric water source (Post et al., 2013). Potential fluid sources with chloride content higher than seawater include the residual water from clay membrane ion filtration, formation of clay minerals, and/or contribution from a brine (Kastner et al., 1991). Brine production in Storfjorden (Fig. 1a) has been documented from CTD data (Skogseth et al., 2005) and the ratio of agglutinated and calcareous foraminifera in the sediment records (Rasmussen and Thomsen 2014). Such brine might explain the elevated chloride concentration. However, the exact causes of the variations in chloride concentration observed in

cores 1522GC and 920GC are not clear at present and await further investigation. For the three sites where gas hydrates were recovered (911GC, 1520GC, and 1521GC), chloride concentrations are scattered around the seawater value, likely reflecting gas hydrate formation/dissociation.

We observed large variations in lithium and strontium concentrations as well as strontium isotopic ratios across the investigated sites. The lithium concentration decreases with depth at the two sites with the deepest SMTZ (1522GC and 940GC; Fig. 2) whereas the concentration stays close to a seawater value at the sites with the shallowest SMTZ (911GC, 1520GC, and 1521GC; Fig. 2). Porewater lithium concentrations increase up to double seawater value at 920GC (Fig. 2), where the SMTZ is at intermediate depth. Strontium concentrations at most of the sites decrease from the seawater value to a minimum at the depth of SMTZ due to the intensive precipitation of authigenic carbonates (Hong et al., 2017) and remain below the seawater concentration throughout the rest of cores (Fig. 2). Only at 920GC, strontium concentrations significantly increase in the deepest three samples. The $^{87}Sr/^{86}Sr$ ratio increases from a seawater value of 0.709217 downcore at the three sites with deeper SMTZ (1522GC, 940GC, and 920GC) whereas the ratios are slightly lower than seawater value throughout the cores at the sites with shallow SMTZ (911GC, 1520GC, and 1521GC).

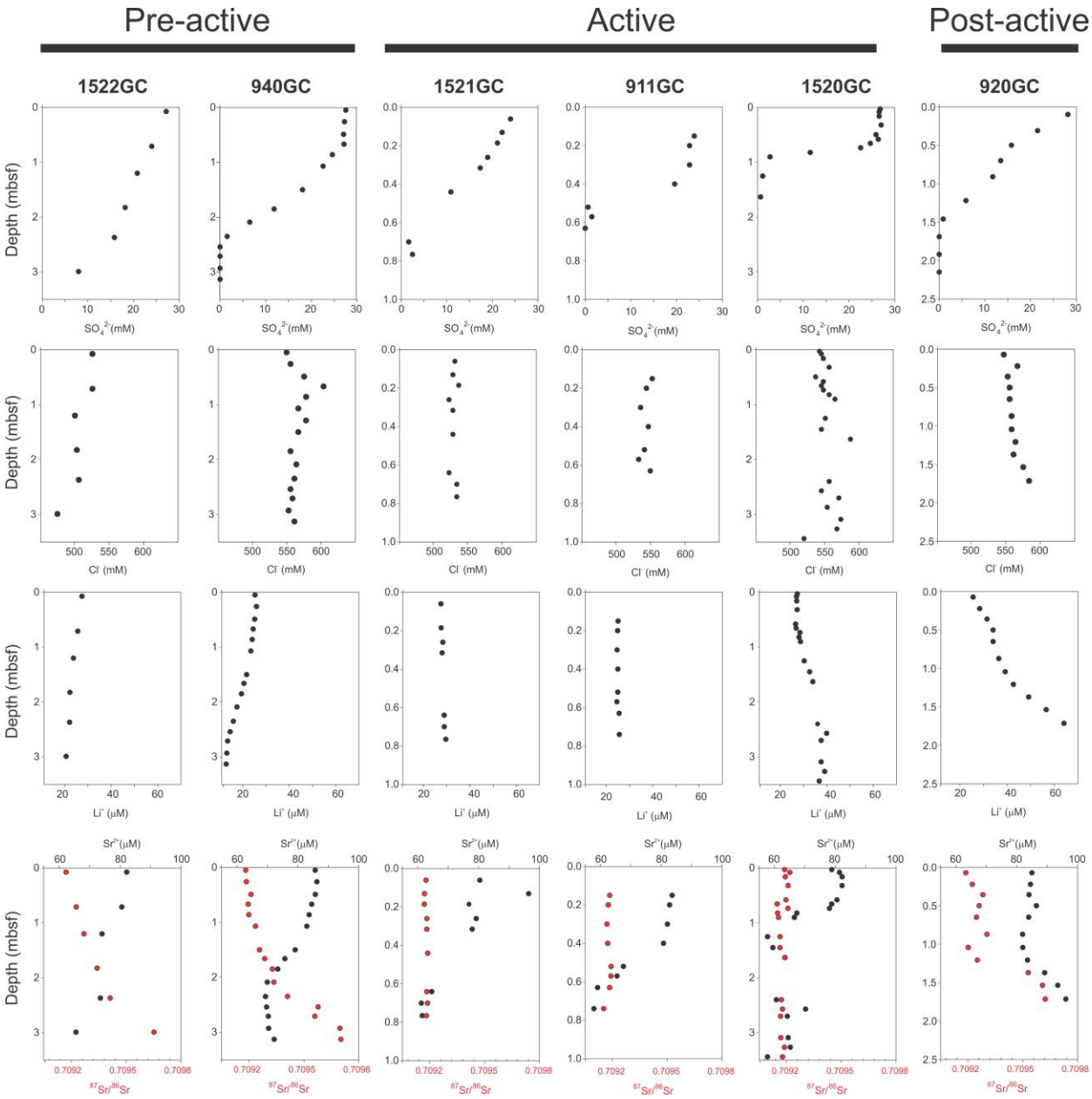

Figure 2: Porewater data from the six investigated sites. The sites were arranged based on the proposed evolution of the seepage (see text for more details).

4.1 Multiple fluid sources inferred from porewater geochemistry

We observed distinct grouping of values among the investigated sites when we compared the $^{87}Sr/^{86}Sr$ ratios against Li/Cl in Fig. 3a and against the inverse of strontium concentrations in Fig. 3b. At sites with low methane flux (grey area in Fig. 3), the strontium concentrations lower than the seawater value (88 μM) are due to intense carbonate precipitation whereas the high

$^{87}Sr/^{86}Sr$ ratios in the pore water (up to 0.7099 and 0.7098 at 1522GC and 940GC, respectively; Fig. 3a) are indicative of ongoing weathering of silicate minerals in marine sediments (i.e., marine silicate weathering or MSiW hereafter). It has been shown that MSiW occurs in the microbial methanogenesis zone due to the lowering of pH associated with fermentation and resulting CO_2 production (Wallmann et al., 2008; Solomon et al., 2014; Kim et al., 2016). The release of strontium due to MSiW is however consumed by the incorporation of strontium into authigenic carbonates (Solomon et al., 2014); so that the resulting data plots are as observed in Fig. 3b. The decreases in both lithium concentrations and Li/Cl ratios in deeper sediments (Figs. 2 and 3) can be explained by the incorporation of lithium into newly formed clay minerals during MSiW (Wallmann et al., 2008; Solomon et al., 2014) or during reverse weathering (Stoffyn-Egli and Mackenzie 1984). Even though the exact mechanism is uncertain, our observations are consistent with lithium consumption by clay minerals at relatively low temperature, as observed elsewhere (Stoffyn-Egli and Mackenzie 1984; Wallmann et al., 2008; Solomon et al., 2014).

In contrast to the sites with low methane supply, site 920GC displays significant enrichments in lithium and strontium concentrations and high $^{87}Sr/^{86}Sr$ in the deepest three samples (blue area in Fig. 3). It is worth noticing that this site is also characterized by high chloride concentration in the fluids (Fig. 2), but the increase in lithium is higher than can be attributed uniquely to a brine source (i.e., high Li/Cl ratios in Fig. 3). Similar to 940GC and 1522GC, the high $^{87}Sr/^{86}Sr$ ratios can be explained by MSiW, but this reaction cannot explain the elevated lithium content, as no such enrichment was observed at other sites where MSiW is confirmed (Solomon et al., 2014; Kim et al., 2016) nor was it observed in 1522GC and 940GC. Lithium can be released through cation exchange with ammonium under relatively low temperatures (e.g., Chan and Kastner 2000). The ammonium concentration at 920GC is below 150 μM throughout the core (Hong et al., 2017), a concentration too low to have significant cation exchange with lithium. Additional lithium sources include hydrothermal activity (Stoffyn-Egli and Mackenzie 1984), opal-A to opal-CT transformation (Gieskes et al., 1982), interaction with the underlying oceanic and continental crust (Martin et al., 1991; You et al., 1995), and release from clays at high temperature (James et al., 2003). We therefore conclude that the high lithium concentration from 920GC must relate to the water-rock interactions at greater depth (You et al., 1995).

191 At the sites with shallow SMTZ (911GC, 1520GC, and 1521GC), both lithium content
192 and $^{87}Sr/^{86}Sr$ are close to seawater values (green areas in Fig. 3), i.e., the pore fluids at these sites
193 present no evidence of MSiW, ion exchange, and/or high temperature water-rock interactions.
194 The lack of any indication of aqueous fluid originated from the microbial methanogenesis zone
195 and deeper is rather unexpected as active seepages are often associated with a water flux sourced
196 from the deep sub-surface (e.g., Haese et al., 2003; Hensen et al., 2004; 2007). We interpret these
197 cation and isotopic signatures to reflect decoupled transport of gaseous and aqueous phases.
198 Multiple lines of evidence indicate that the high methane supply at these sites is sustained by a
199 gaseous phase. Hong et al., (2017) reported the recovery of shallow gas hydrates which
200 necessitates a gaseous methane source (Bohrmann et al., 1998; Torres et al., 2004; Liu and
201 Flemings 2006; Sultan et al., 2014). Persistent gas plumes in the water column were observed
202 above these active sites (Serov et al., 2017) at locations where amplitude anomalies indicative of
203 gas accumulation at depth are persistent in the seismic profile (Fig. 1c). The stable isotopic
204 signatures from a gas sample taken directly from the bubbles in the water column reveal the
205 thermogenic origin of the gas (-47.7‰ and -242‰ for $\delta^{13}C\text{-}CH_4$ and $\delta D\text{-}CH_4$, respectively). As
206 this gas pulse moves upward, it saturates the pore space, hinders aqueous advection (Mogollón et
207 al., 2009), and potentially minimizes the diffusion of solutes other than methane, which
208 altogether explains the lack of evidence for chemically altered fluid observed below SMTZ at
209 these active sites.
210

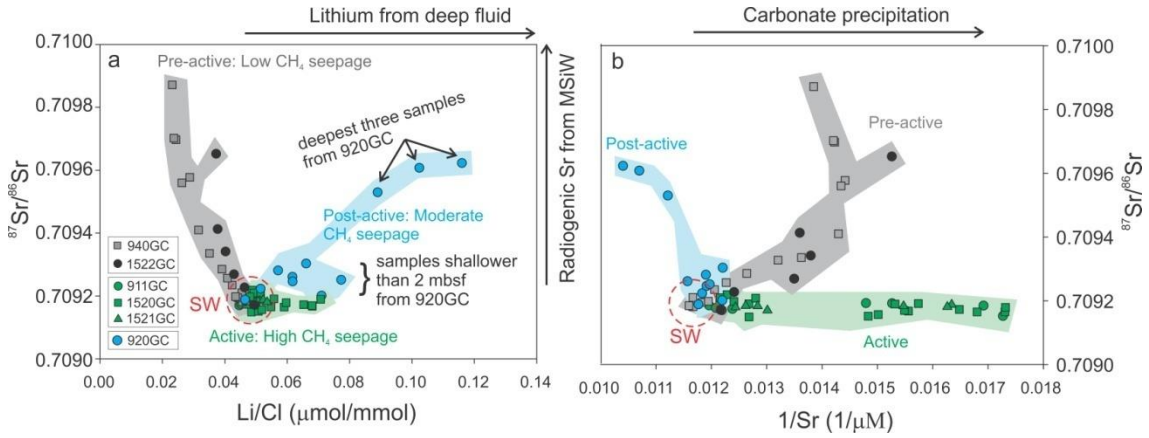

211

Figure 3: Cross-plot of (a) Sr isotope vs. Li/Cl ratios and (b) Sr isotopes versus 1/Sr. See text for explanation of each end members.

4.2 Different fluid transport modes during the three seepage stages

The contrasting geochemical patterns observed in the six investigated sites do not only reflect the complex diagenetic processes and different fluid sources present in this margin, but point to a decoupled transport of water and gas among the different GHMs. Such decoupling between aqueous and gaseous phases has been previously proposed to explain positive porewater chloride anomalies observed at numerous gas hydrate-bearing sites worldwide (Torres et al., 2004; Liu and Flemings 2006; Daigle and Dugan 2010; Daigle et al., 2011; Torres et al., 2011; Peszynska et al., 2016). Torres et al. (2004) and Trehu et al. (2004) proposed that the propagation of fractures is enhanced by the excess pore pressure associated with gaseous methane. Liu and Flemings (2006) and Daigle and Dugan (2010) proposed that gaseous methane migrates into the gas hydrate stability zone along a local three-phase equilibrium driven by rapid gas hydrate formation with the resultant high porewater salinity. Despite the different mechanisms proposed, a decoupled migration of gaseous and aqueous phases is well established. Pore space saturated with a gas phase precludes the upward migration of the aqueous phase due to its smaller relative permeability (Lee 2008). Such interpretation is consistent with the modeling of porewater profiles at 911GC by Hong et al. (2017), who concluded that the advection of aqueous phase is absent at the active sites and diffusion is the main transport mechanism for solutes.

We argue that the observed decoupling of gaseous and aqueous phases in the GHMs reflects the different seepage stages. Based on all our geochemical and geophysical observations, we propose the following three-stage evolution model for Storfjordrenna GHMs (Fig. 4). For sites representing the first stage prior to initiation of gas advection ("pre-active stage" in Figs. 4a&4b), solute transport is governed by diffusion. During this stage, the pore fluids are influenced by MSiW within the methanogenesis zone, i.e., below SMTZ. The release of strontium during MSiW is mostly consumed by authigenic carbonate precipitation while the high $^{87}Sr/^{86}Sr$ signals are preserved and observed from 940GC and 1522GC. Lithium at these sites is incorporated into clay minerals which results in the concentrations lower than the seawater value. Methane flux is low as the flux is sustained by the inefficient solute diffusion.

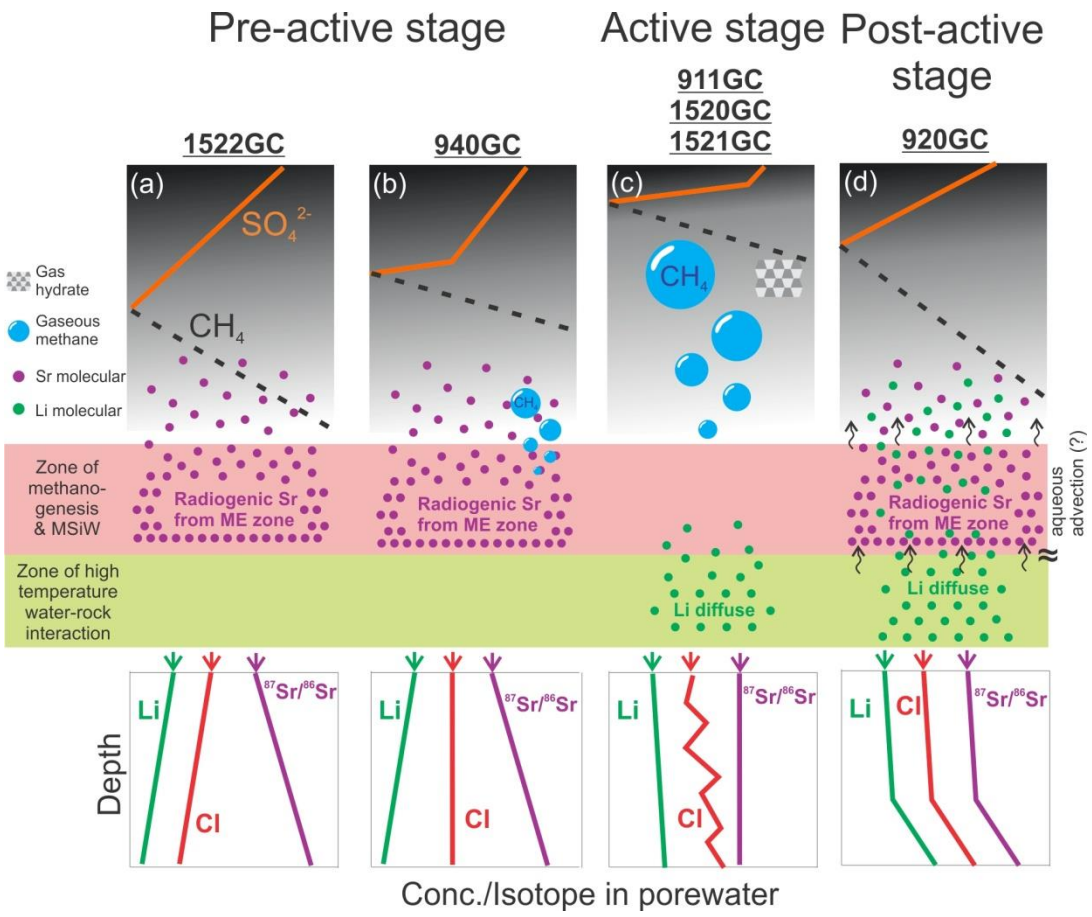

Figure 4: We propose that the decoupled transport between gaseous and aqueous phases is related to the different life stages of the investigated GHMs. (a) Methane is transported primarily by diffusion during the pre-active stage which explains the smooth sulfate profile observed from 1522GC. (b) At the end this stage, ascending of gaseous methane induces rapid sulfate consumption through AOM . As the consumption rate is much faster than sulfate diffusion, we observed a non-steady state sulfate profile from 940GC. (c) During the active stage, the methane supply is sustained by a gaseous phase which can be mapped by our seismic data in the sediments (Fig. 1c). The lack of geochemical proxies for deep aqueous fluid indicates aqueous advection is mostly absent during this stage. (d) During post-active stage, when the free gas reservoir is exhausted, aqueous advection becomes the primarily transport mode carrying methane and other trace elements (e.g., Li) from the greater depth. Contrasting to the sites in the active stage, no gas hydrate was recovered in the first few meters of sediments as dissolved methane is now delivered inefficiently to the shallow sub-surface.

The most active stage of the seepage is initiated when the gaseous reservoir is tapped ("active stage" in Fig. 4c), possibly driven by hydrofracturing the formation when gas content is high enough to generate the required overpressure (Daigle and Dugan 2010). Methane is then delivered by the gas advection to the shallow subsurface which results in the non-steady-state profiles (e.g., 911GC and 1520GC) and promotes the precipitation of shallow gas hydrate (Hong et al., 2017). The gaseous methane discharges at the seafloor in the form of bubble plumes as has been documented by the hydroacoustic surveys (Serov et al., 2017). Gas in the venting bubbles is thermogenic by origin as confirmed by their stable isotopic signature (Fig. 1c). It is likely that the fracture systems underlying the study area provide pathways for deep-sourced gas to migrate upward (Fig. 1d), as documented by Mau et al. (2017). During this stage, the transport of gaseous and aqueous phases is decoupled. While methane gas is rapidly ascending, aqueous flow is restricted and solutes in the porewater are only inefficiently transported by diffusion. Such decoupling explains why neither a significant $^{87}Sr/^{86}Sr$ ratios nor changes in lithium concentrations are observed at the active sites.

In response to the exhaustion of a subsurface gaseous reservoir, delivery of gaseous methane terminates ("post-active stage" in Fig. 4d). We propose that the draining of the gas reservoir generates low pressures that induces the advection of a deep aqueous phase as inferred from both the high concentration of dissolved Li and the concave-upward shape of the Li porewater profile at 920GC (Fig. 2). The geochemical signal of MSiW (e.g., high $^{87}Sr/^{86}Sr$ ratios) is clearly delivered to the shallow sediments by the ascending aqueous phase. We modified the reduced 1-D model of Hong et al. (2017) and estimated that an advection rate of ca. 1 cm/yr is required to produce the observed lithium profile at this site (see Supplementary Information for more modeling details). Such rate is lower than the advection rates from seep sites with known focused fluid flow such as Hydrate Ridge (50-100 cm/yr; Torres et al., 2002), Black Sea (8-25 cm/yr; Wallmann et al., 2006), and Bush Hill in the Gulf of Mexico (up to several hundreds of cm/yr; Solomon et al., 2008). We propose that GHM5 reflects the post-active phase of seepage, which contrasts the other four active GHMs in the region (Fig. 1b). This inference is supported by the observations that GHM5 is the only mound where no hydroacoustic flares have been detected over the past 3 years of surveys and no gas hydrate was recovered during repeated gravity coring.

It is noted that the availability of gaseous methane and the development of conduits for methane transport largely determine the seepage evolution. Therefore, if a gas supply or a conduit below any of the pre-active sites is not in place, the site will never proceed to the next stage. Similarly, if the pore pressure gradient in the sediment column is too small to drive the advection of aqueous phase, diffusion will be the primary process governing the distribution of solutes at the post-active stage. Such dependency on the pressure condition of the underlying fluid flow system is reflected by the spatial heterogeneity of seepage as observed by Hong et al. (2017) and could be explained by our proposed three-state evolution model.

5 Conclusions

We compiled observations from porewater geochemistry and geophysical data to document a decoupled fluid transport and evolution of a seepage system in Storfjordrenna, a marine Arctic cold seep. We showed that different fluid transport modes across three life stages (diffusion, gaseous advection, and aqueous advection) characterize the temporal evolution of seepage from the investigated GHMs:

1) A pervasive signal of high $^{87}Sr/^{86}Sr$ ratios in the porewater documents silicate weathering in the microbial methanogenic zone of the sediments. The results of such weathering are neo formation of clay minerals and adsorption of alkali metals such as lithium. Solutes, as well as dissolved methane, are transported primarily by diffusion, which explains the low methane flux and deep SMTZ. This set of condition characterizes the system prior to the initiation of seepage.
2) The initiation of a methane pulse is characterized by rapid advection of gaseous thermogenic methane, which sustains the vigorous bubbling at the seafloor and the formation of massive gas hydrate in the shallow sediments, a similar mechanism as previously proposed (Torres et al., 2004; Liu and Flemings 2006). Despite the active gas advection, there is no evidence of deep aqueous fluid at this stage as indicated by the seawater-like composition of fluid. These observations can be explained by a decoupled transport of gaseous and aqueous phases, and the barrier of aqueous flow imposed by the low permeability that develops when gas occupies the sediment pore space.

3) After the exhaustion of the gaseous reservoir and the cessation of active gas discharge at the seafloor, a newly generated low pressure induces the advection of the aqueous phase which results in the high lithium concentration observed from the site representing such post-active stage. Based on the lithium profile, we estimated that the aqueous advection rate is around 1 cm/yr at the investigated site.

Acknowledgments, Samples, and Data

All geochemical data reported in the paper are included in the Dataset S1 of the Supporting material. We would like to acknowledge the captains and crews onboard R/V Helmer Hanssen. We acknowledge Haoyi Yao for preparing the bathymetry map (Fig. 1b) and the sampling work during the cruises. This work was supported by the Research Council of Norway through its Centres of Excellence funding scheme (project number 223259), NORCRUST (project number 255150) as well as by the US Department of Energy (DE-FE0013531). We declare no conflict of interest for any coauthors. We also acknowledge Dr. Xiaoli Liu and another anonymous reviewer for their constructive comments which have substantially enhance the quality of the paper.

3996 words (7.99 PU) + 4 figures = 11.99 PU (limit: 12 PU)

Captions

Figure 1: (a) A regional map showing the study area and the location of the deep seismic profile in (d). (b) Detailed bathymetry map showing the investigated sediment cores. We focused on the completed dataset from the six sites (larger label fonts in (b)) and showed available data for the other six sites (smaller label fonts in (b)) in the Supplementary information. The red line (x-y-z) marks the location of the P-Cable seismic line in (c) across the two investigated GHMs with the stable isotopic signatures of a gas bubble sample collected. (d) Structural geological profile (modified after Engen et al., 2008) showing the location of the two major fault systems in relation to Storfjordrenna GHMs.

Figure 2: Porewater data from the six investigated sites. The sites were arranged based on the proposed evolution of the seepage (see text for more details).

Figure 3: Cross-plot of (a) Sr isotope vs. Li/Cl ratios and (b) Sr isotopes versus 1/Sr. See text for explanation of each end members.

Figure 4: We propose that the decoupled transport between gaseous and aqueous phases is related to the different life stages of the investigated GHMs. (a) Methane is transported primarily by diffusion during the pre-active stage which explains the smooth sulfate profile observed from 1522GC. (b) At the end of the pre-active stage, ascending of gaseous methane induces rapid sulfate consumption through AOM. As the rate is much faster than sulfate diffusion, we observed a non-steady state sulfate profile from 940GC. (c) During the active stage, the methane supply is sustained by a gaseous phase which can be mapped by our seismic data in the sediments (Fig. 1c). The lack of geochemical proxies for deep aqueous fluid indicates aqueous advection is mostly absent during this stage. (d) During post-active stage, when the free gas reservoir is exhausted, aqueous advection becomes the primarily transport mode carrying methane and other trace elements (e.g., Li) from the greater depth. Contrasting to the sites in the active stage, no gas hydrate was recovered in the first few meters of sediments as dissolved methane is now delivered inefficiently to the shallow sub-surface.

References

Andersen, E. S., T. M. Dokken, A. Elverhøi, A. Solheim and I. Fossen (1996). "Late quaternary sedimentation and glacial history of the western Svalbard continental margin." Marine Geology **133**(3): 123-156.

Boetius, A. and F. Wenzhofer (2013). "Seafloor oxygen consumption fuelled by methane from cold seeps." Nature Geoscience **6**(9): 725-734.

Bohrmann, G., J. Greinert, E. Suess and M. Torres (1998). "Authigenic carbonates from the Cascadia subduction zone and their relation to gas hydrate stability." Geology **26**(7): 647-650.

Breivik, A. J., R. Mjelde, P. Grogan, H. Shimamura, Y. Murai and Y. Nishimura (2003). "Crustal structure and transform margin development south of Svalbard based on ocean bottom seismometer data." Tectonophysics **369**(1): 37-70.

Chan, L.-H. and M. Kastner (2000). "Lithium isotopic compositions of pore fluids and sediments in the Costa Rica subduction zone: implications for fluid processes and sediment contribution to the arc volcanoes." Earth And Planetary Science Letters **183**(1): 275-290.

Daigle, H., N. L. Bangs and B. Dugan (2011). "Transient hydraulic fracturing and gas release in methane hydrate settings: A case study from southern Hydrate Ridge." Geochemistry Geophysics Geosystems **12**.

Daigle, H. and B. Dugan (2010). "Effects of multiphase methane supply on hydrate accumulation and fracture generation." Geophysical Research Letters **37**.

Elverhøi, A. and A. Solheim (1983). "The Barents Sea ice sheet-a sedimentological discussion." Polar Research **1**(1): 23-42.

Engen, Ø., J. I. Faleide and T. K. Dyreng (2008). "Opening of the Fram Strait gateway: a review of plate tectonic constraints." Tectonophysics **450**(1): 51-69.

Gabrielsen, R. (1984). "Long-lived fault zones and their influence on the tectonic development of the southwestern Barents Sea." Journal of the Geological Society **141**(4): 651-662.

Gieskes, J. M., H. Elderfield, J. R. Lawrence, J. Johnson, B. Meyers and A. Campbell (1982). "16. Geochemistry Of Interstitial Waters And Sediments, Leg 64, Gulf Of California1." Initial Reports of the Deep Sea Drilling Project: A Project Planned by and Carried Out with the Advice of the Joint Oceanographic Institutions for Deep Earth Sampling **64**: 675.

Greinert, J., K. Lewis, J. Bialas, I. A. Pecher, A. Rowden, D. Bowden, M. De Batist and P. Linke (2010). "Methane seepage along the Hikurangi Margin, New Zealand: Overview of studies in 2006 and 2007 and new evidence from visual, bathymetric and hydroacoustic investigations." Marine Geology **272**(1): 6-25.

Greinert, J., M. Veloso, M. A. De Batist and J. Mienert (2013). Hydroacoustic quantification of free-gas venting offshore Svalbard, Arctic: Changes in space and time. AGU Fall Meeting Abstracts.

Haeckel, M., E. Suess, K. Wallmann and D. Rickert (2004). "Rising methane gas bubbles form massive hydrate layers at the seafloor." Geochimica et Cosmochimica Acta **68**(21): 4335-4345.

Haese, R. R., C. Meile, P. Van Cappellen and G. J. De Lange (2003). "Carbon geochemistry of cold seeps: Methane fluxes and transformation in sediments from Kazan mud volcano, eastern Mediterranean Sea." Earth and Planetary Science Letters **212**(3-4): 361-375.

Haydon, P. R. and D. L. Graf (1986). "Studies of smectite membrane behavior: temperature dependence, 20–180 C." Geochimica Et Cosmochimica Acta **50**(1): 115-121.

Hensen, C., K. Wallmann, M. Schmidt, V. Liebetrau, U. Fehn, D. Garbe-Schonberg and W. Bruckmann (2007). "Geochemistry of cold vent fluids at the Central American Convergent Margin." Geochimica Et Cosmochimica Acta **71**(15): A396-A396.

Hensen, C., K. Wallmann, M. Schmidt, C. R. Ranero and E. Suess (2004). "Fluid expulsion related to mud extrusion off Costa Rica - A window to the subducting slab." Geology **32**(3): 201-204.

Hong, W. L., M. E. Torres, J. Carroll, A. Cremiere, G. Panieri, H. Yao and P. Serov (2017). "Seepage from an Arctic shallow marine gas hydrate reservoir is insensitive to momentary ocean warming." Nature communications.

Hovland, M., A. G. Judd and R. A. Burke (1993). "The global flux of methane from shallow submarine sediments." Chemosphere **26**(1): 559-578.

Ingólfsson, Ó. and J. Y. Landvik (2013). "The Svalbard–Barents Sea ice-sheet – Historical, current and future perspectives." Quaternary Science Reviews **64**: 33-60.

James, R. H., D. E. Allen and W. E. Seyfried (2003). "An experimental study of alteration of oceanic crust and terrigenous sediments at moderate temperatures (51 to 350°C): insights as to chemical processes in near-shore ridge-flank hydrothermal systems." Geochimica Et Cosmochimica Acta **67**(4): 681-691.

Kastner, M., H. Elderfield and J. B. Martin (1991). "Fluids in Convergent Margins: What do We Know about their Composition, Origin, Role in Diagenesis and Importance for Oceanic Chemical Fluxes?" Philosophical Transactions: Physical Sciences and Engineering **335**(1638): 243-259.

Kim, J.-H., M. E. Torres, W.-L. Hong, J. Choi, M. Riedel, J. J. Bahk and S.-H. Kim (2013a). "Pore fluid chemistry from the Second Gas Hydrate Drilling Expedition in the Ulleung Basin (UBGH2): Source, mechanisms and consequences of fluid freshening in the central part of the Ulleung Basin, East Sea." Marine and Petroleum Geology **47**: 99-112.

Kim, J. H., M. E. Torres, B. A. Haley, J. S. Ryu, M. H. Park, W. L. Hong and J. Choi (2016). "Marine silicate weathering in the anoxic sediment of the Ulleung Basin: Evidence and consequences." Geochemistry, Geophysics, Geosystems **17**(8): 3437-3453.

Kvenvolden, K. A. and B. W. Rogers (2005). "Gaia's breath - global methane exhalations." Marine and Petroleum Geology **22**(4): 579-590.

Lee, M. W. (2008). Models for gas hydrate-bearing sediments inferred from hydraulic permeability and elastic velocities. Scientific Investigations Report 2008–5219, U.S. Department of the Interior
U.S. Geological Survey**:** 14p.

Liu, X. L. and P. B. Flemings (2006). "Passing gas through the hydrate stability zone at southern Hydrate Ridge, offshore Oregon." Earth And Planetary Science Letters **241**(1-2): 211-226.

MacDonald, I., N. Guinasso, R. Sassen, J. Brooks, L. Lee and K. Scott (1994). "Gas hydrate that breaches the sea floor on the continental slope of the Gulf of Mexico." Geology **22**(8): 699-702.

Martin, J. B., M. Kastner and H. Elderfield (1991). "Lithium: sources in pore fluids of Peru slope sediments and implications for oceanic fluxes." Marine Geology **102**(1): 281-292.

Mau, S., M. Römer, M. Torres, I. Bussmann, T. Pape, E. Damm, P. Geprägs, P. Wintersteller, C.-W. Hsu and M. Loher (2017). "Widespread methane seepage along the continental margin off Svalbard-from Bjørnøya to Kongsfjorden." Scientific Reports **7**.

Mogollón, J. M., I. L'Heureux, A. W. Dale and P. Regnier (2009). "Methane gas-phase dynamics in marine sediments: A model study." American Journal of Science **309**(3): 189-220.

Myhre, A. M., O. Eldholm and E. Sundvor (1982). "The margin between Senja and Spitsbergen fracture zones: implications from plate tectonics." Tectonophysics **89**(1-3): 33-50.

Mörner, N.-A. (1978). "Faulting, fracturing, and seismicity as functions of glacio-isostasy in Fennoscandia." Geology **6**(1): 41-45.

Nikolovska, A., H. Sahling and G. Bohrmann (2008). "Hydroacoustic methodology for detection, localization, and quantification of gas bubbles rising from the seafloor at gas seeps from the eastern Black Sea." Geochemistry, Geophysics, Geosystems **9**(10).

Patton, H., A. Hubbard, K. Andreassen, M. Winsborrow and A. P. Stroeven (2016). "The build-up, configuration, and dynamical sensitivity of the Eurasian ice-sheet complex to Late Weichselian climatic and oceanic forcing." Quaternary Science Reviews **153**: 97-121.

Peszynska, M., W.-L. Hong, M. E. Torres and J.-H. Kim (2016). "Methane Hydrate Formation in Ulleung Basin Under Conditions of Variable Salinity: Reduced Model and Experiments." Transport in Porous Media: 1-27.

Petersen, C. J., S. Bünz, S. Hustoft, J. Mienert and D. Klaeschen (2010). "High-resolution P-Cable 3D seismic imaging of gas chimney structures in gas hydrated sediments of an Arctic sediment drift." Marine and Petroleum Geology **27**(9): 1981-1994.

Post, V. E., J. Groen, H. Kooi, M. Person, S. Ge and W. M. Edmunds (2013). "Offshore fresh groundwater reserves as a global phenomenon." Nature **504**(7478): 71-78.

Rasmussen, T. and E. Thomsen (2014). "Brine formation in relation to climate changes and ice retreat during the last 15,000 years in Storfjorden, Svalbard, 76–78 N." Paleoceanography **29**(10): 911-929.

Reeburgh, W. S. (2007). "Oceanic methane biogeochemistry." Chemical Reviews **107**(2): 486-513.

Regnier, P., A. W. Dale, S. Arndt, D. E. LaRowe, J. Mogollon and P. Van Cappellen (2011). "Quantitative analysis of anaerobic oxidation of methane (AOM) in marine sediments: A modeling perspective." Earth-Science Reviews **106**(1-2): 105-130.

Römer, M., H. Sahling, T. Pape, A. Bahr, T. Feseker, P. Wintersteller and G. Bohrmann (2012). "Geological control and magnitude of methane ebullition from a high-flux seep area in the Black Sea—the Kerch seep area." Marine Geology **319–322**: 57-74.

Sahling, H., M. Römer, T. Pape, B. Bergès, C. dos Santos Fereirra, J. Boelmann, P. Geprägs, M. Tomczyk, N. Nowald and W. Dimmler (2014). "Gas emissions at the continental margin west off Svalbard: mapping, sampling, and quantification." Biogeosciences Discussions **11**: 7189-7234.

Sauter, E. J., S. I. Muyakshin, J. L. Charlou, M. Schluter, A. Boetius, K. Jerosch, E. Damm, J. P. Foucher and M. Klages (2006). "Methane discharge from a deep-sea submarine mud volcano into the upper water column by gas hydrate-coated methane bubbles." Earth and Planetary Science Letters **243**(3-4): 354-365.

Serov, P., S. Vadakkepuliyambatta, J. Mienert, H. Patton, A. Portnov, A. Silyakova, G. Panieri, M. L. Carroll, J. Carroll, K. Andreassen and A. Hubbard (2017). "Postglacial response of Arctic Ocean gas hydrates to climatic amelioration." Proceedings of the National Academy of Sciences **114**(24): 6215-6220.

Skogseth, R., P. M. Haugan and M. Jakobsson (2005). "Watermass transformations in Storfjorden." Continental Shelf Research **25**(5–6): 667-695.

Smith, A. J., J. Mienert, S. Bunz and J. Greinert (2014). "Thermogenic methane injection via bubble transport into the upper Arctic Ocean from the hydrate-charged Vestnesa Ridge, Svalbard." Geochemistry Geophysics Geosystems **15**(5): 1945-1959.

Solomon, E. A., M. Kastner, H. Jannasch, G. Robertson and Y. Weinstein (2008). "Dynamic fluid flow and chemical fluxes associated with a seafloor gas hydrate deposit on the northern Gulf of Mexico slope." Earth and Planetary Science Letters **270**(1): 95-105.

Solomon, E. A., A. J. Spivack, M. Kastner, M. E. Torres and G. Robertson (2014). "Gas hydrate distribution and carbon sequestration through coupled microbial methanogenesis and silicate weathering in the Krishna–Godavari Basin, offshore India." Marine and Petroleum Geology **58, Part A**: 233-253.

Solomon, E. A., A. J. Spivack, M. Kastner, M. E. Torres and G. Robertson (2014). "Synthesis of pore fluid geochemistry in the Krishna-Godavari Basin - Gas hydrate distribution and carbon sequestration through coupled microbial methanogenesis and silicate weathering." Marine and Petroleum Geology **(Submitted)**.

Stewart, I. S., J. Sauber and J. Rose (2000). "Glacio-seismotectonics: ice sheets, crustal deformation and seismicity." Quaternary Science Reviews **19**(14–15): 1367-1389.

Stoffyn-Egli, P. and F. T. Mackenzie (1984). "Mass balance of dissolved lithium in the oceans." Geochimica Et Cosmochimica Acta **48**(4): 859-872.

Sultan, N., G. Bohrmann, L. Ruffine, T. Pape, V. Riboulot, J. L. Colliat, A. De Prunele, B. Dennielou, S. Garziglia and T. Himmler (2014). "Pockmark formation and evolution in deep water Nigeria: Rapid hydrate growth versus slow hydrate dissolution." Journal of Geophysical Research: Solid Earth **119**(4): 2679-2694.

Sundvor, E. and O. Eldholm (1976). Marine geophysical survey on the continental margin from Bear Island to Hornsund, Spitsbergen, Observatory, Univ.

Torres, M. E., J.-H. Kim, J.-Y. Choi, B.-J. Ryu, J.-J. Bahk, M. Riedel, T. Collett, W.-L. Hong and M. Kastner (2011). Occurrence of High Salinity Fluids Associated with Massive Near-seafloor Gas Hydrate Deposits. 7th International Conference on Gas Hydrates. Edinburgh, Scotland, United Kingdom.

Torres, M. E., J. McManus, D. E. Hammond, M. A. de Angelis, K. U. Heeschen, S. L. Colbert, M. D. Tryon, K. M. Brown and E. Suess (2002). "Fluid and chemical fluxes in and out of sediments hosting methane hydrate deposits on Hydrate Ridge, OR, I: Hydrological provinces." Earth And Planetary Science Letters **201**(3-4): 525-540.

Torres, M. E., K. Wallmann, A. M. Trehu, G. Bohrmann, W. S. Borowski and H. Tomaru (2004). "Gas hydrate growth, methane transport, and chloride enrichment at the southern summit of Hydrate Ridge, Cascadia margin off Oregon." Earth and Planetary Science Letters **226**(1-2): 225-241.

Trehu, A. M., P. B. Flemings, N. L. Bangs, J. Chevallier, E. Gracia, J. E. Johnson, C. S. Liu, X. L. Liu, M. Riedel and M. E. Torres (2004). "Feeding methane vents and gas hydrate deposits at south Hydrate Ridge." Geophysical Research Letters **31**(23).

Ussler, W. and C. K. Paull (2001). Ion Exclusion Associated with Marine Gas Hydrate Deposits. Natural Gas Hydrates: Occurrence, Distribution, and Detection, American Geophysical Union**:** 41-51.

Wallmann, K., G. Aloisi, M. Haeckel, P. Tishchenko, G. Pavlova, J. Greinert, S. Kutterolf and A. Eisenhauer (2008). "Silicate weathering in anoxic marine sediments." Geochimica et Cosmochimica Acta **72**(12): 2895-2918.

Wallmann, K., M. Drews, G. Aloisi and G. Bohrmann (2006). "Methane discharge into the Black Sea and the global ocean via fluid flow through submarine mud volcanoes." Earth and Planetary Science Letters **248**(1-2): 545-560.

Wegner, C., K. E. Bennett, A. de Vernal, M. Forwick, M. Fritz, M. Heikkilä, M. Łącka, H. Lantuit, M. Laska and M. Moskalik (2015). "Variability in transport of terrigenous material on the shelves and the deep Arctic Ocean during the Holocene." Polar Research **34**(1): 24964.

You, C.-F., L. Chan, A. Spivack and J. Gieskes (1995). "Lithium, boron, and their isotopes in sediments and pore waters of Ocean Drilling Program Site 808, Nankai Trough: implications for fluid expulsion in accretionary prisms." Geology **23**(1): 37-40.

National Energy Technology Laboratory

626 Cochrans Mill Road
P.O. Box 10940
Pittsburgh, PA 15236-0940

3610 Collins Ferry Road
P.O. Box 880
Morgantown, WV 26507-0880

13131 Dairy Ashford Road, Suite 225
Sugar Land, TX 77478

1450 Queen Avenue SW
Albany, OR 97321-2198

Arctic Energy Office
420 L Street, Suite 305
Anchorage, AK 99501

Visit the NETL website at:
www.netl.doe.gov

Customer Service Line:
1-800-553-7681

NATIONAL ENERGY TECHNOLOGY LABORATORY

U.S. DEPARTMENT OF ENERGY | NATIONAL ENERGY TECHNOLOGY LABORATORY